J. Fluid Mech. (1989), *vol.* 199, *pp.* 281–296
Printed in Great Britain

Shock splitting in single-phase gases

By M. S. CRAMER

Department of Engineering Science & Mechanics, Virginia Polytechnic Institute & State University, Blacksburg, VA 24061, USA

(Received 7 April 1988)

We consider single-phase gases in which the fundamental derivative is negative over a finite range of pressures and temperatures and show that inadmissible discontinuities give rise to shock splitting. The precise conditions under which splitting occurs are delineated and the formation of the split-shock configuration from smooth initial conditions is described. Specific numerical examples of shock splitting are also provided through use of exact inverse solutions.

1. Introduction

Bethe (1942) and Zel'dovich (1946) were the first to discuss the possibility of expansion shocks in single-phase fluids. Expansion shocks are gasdynamic shocks in which the usual entropy increase across the shock requires a decrease, rather than increase, in the pressure and temperature. Such shocks are possible in fluids which have specific heats large enough to cause the fundamental derivative

$$\Gamma(\rho, s) \equiv \frac{a}{\rho}+\frac{\partial a}{\partial \rho}\bigg|_s \tag{1.1}$$

to become negative for a range of temperatures and pressures in the general neighbourhood of the thermodynamic critical point. This region is depicted in figure 1 for the special case of a van der Waals gas with a constant specific heat. In this study we refer to fluids which possess such a region of negative nonlinearity ($\Gamma < 0$) as Bethe–Zel'dovich fluids. An important contribution to the issue of the existence of negative nonlinearity is due to Lambrakis & Thompson (1972) and Thompson & Lambrakis (1973) who employed realistic equations of state to give examples of practical fluids having $\Gamma < 0$ over a finite range of pressures and temperatures.

When Γ is negative for all pressures and temperatures encountered in a particular flow, the wave evolution is seen to be essentially the same as that for $\Gamma > 0$ provided one takes into account the backward steepening and necessity of expansion shocks. Recent studies have shown that the flow can show significant qualitative differences with the $\Gamma > 0$ case if Γ changes sign within the flow; we refer to cases where Γ changes sign as those of mixed nonlinearity. Although mentioned by earlier authors, the first extensive discussion of sonic shocks was given by Thompson & Lambrakis (1973). Sonic shocks are shocks having a speed identically equal to the convected sound speed immediately upstream or downstream of the shock and are not possible if Γ is strictly positive or strictly negative. Cramer & Kluwick (1984), Cramer *et al.* (1986) and Cramer & Sen (1987) have shown that mixed nonlinearity may also result in a partial or total disintegration of both compression and expansion shocks; the partial disintegration results in a sonic shock and centred fan. The complicated dynamics of sonic shocks have also been described by Turner (1979, 1981) in the context of

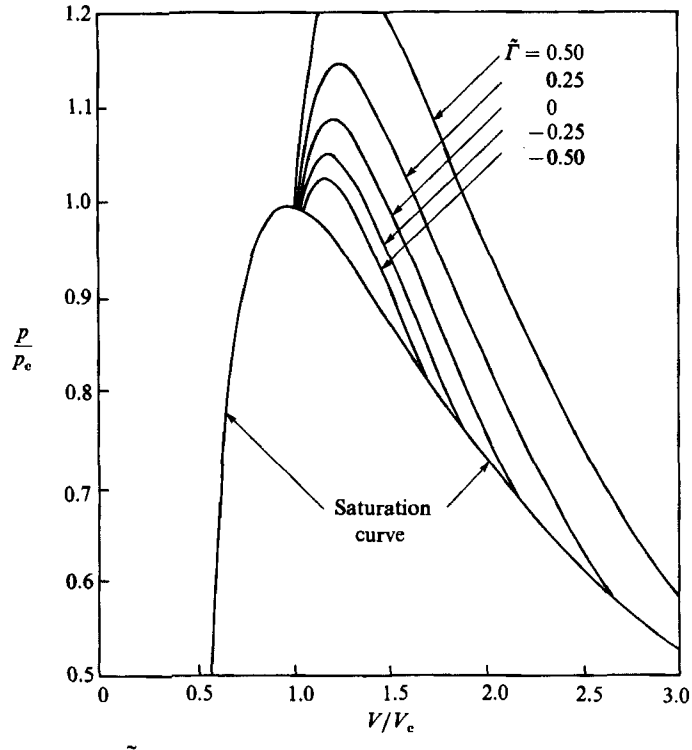

FIGURE 1. Constant $\tilde{\Gamma} = \rho\Gamma/a$ contours for a van der Waals gas with $c_v/R = 50 =$ constant. The subscript c denotes conditions at the thermodynamic critical point.

superfluid helium, by Lee-Bapty (1981) in the context of Kelvin–Voigt solids and Lee-Bapty & Crighton (1987) in the context of a modified Burgers equation.

Cramer & Sen (1986*a*) and Cramer (1987*b*, *c*) have demonstrated that compression shocks of sufficient strength may be subject to shock splitting, i.e. the original discontinuity splits into two sonic shocks separated by an isentropic compression fan. The present paper provides the full description of this phenomenon including its relation to the basic shock admissibility conditions and, in particular, the existence of a dissipative structure.

When Γ is either strictly positive or strictly negative, the entropy inequality is sufficient to rule out inadmissible discontinuities. When Γ changes sign across the proposed discontinuity, the entropy inequality is no longer sufficient and more general conditions must be imposed. Thompson & Lambrakis (1973), Cramer & Kluwick (1984) and Cramer & Sen (1987) employed a speed-ordering relation which required the flow to undergo a supersonic–subsonic transition across the shock. The relation of this condition to the existence of a dissipative structure was discussed by Cramer & Kluwick (1984), Lee-Bapty & Crighton (1987) and Cramer (1987*a*). Cramer (1987*b*) has pointed out that even the speed-ordering relation may not be sufficient when the flow is taken from one side of the region of negative nonlinearity to the other. In particular, discontinuities may be constructed which satisfy the usual inviscid condition, viz. the Rankine–Hugoniot jump conditions, the entropy inequality and the speed-ordering relation, but which do not possess a dissipative structure. This fact is proven in §3 of the present study by inspection of the phase plane of the classical shock structure model.

Once admissibility conditions have been established, the evolution of inadmissible discontinuities are of interest; the present study shows that any complete description of this evolution must involve shock splitting. In §4 we delineate the conditions under which shock splitting occurs in arbitrary Bethe–Zel'dovich fluids and relate this to the partial disintegration of inadmissible shocks described by previous investigators. We also provide a specific numerical example of shock splitting through use of the exact solutions of Cramer & Sen (1987). In §5 we demonstrate that the split-shock configuration is not just possible but will always evolve from smooth initial conditions, at least within the context of the isentropic approximation employed.

The conclusions of this study are obtained from a relatively small collection of key facts. In §2 we summarize these facts along with the fundamental assumptions employed.

2. Formulation and useful identities

We restrict our attention to single-phase Navier–Stokes fluids satisfying the inequalities

$$\mu \geqslant 0, \quad 3\lambda + 2\mu \geqslant 0, \quad k \geqslant 0, \tag{2.1}$$

$$\left.\frac{\partial p}{\partial \rho}\right|_T > 0, \quad c_v > 0, \tag{2.2}$$

$$\beta = -\frac{1}{\rho}\left.\frac{\partial \rho}{\partial T}\right|_p > 0, \tag{2.3}$$

where T, $\mu(\rho,T)$, $\lambda(\rho,T)$, $k(\rho,T)$, $p(\rho,T)$, $c_v(\rho,T)$ and $\beta(\rho,T)$ are the absolute temperature, shear viscosity, second viscosity, thermodynamic pressure, specific heat at constant volume and the coefficient of thermal expansion. The first set (2.1) guarantees that the second law of thermodynamics is always satisfied. The second set (2.2) arises from the requirement of thermodynamic equilibrium. The usual manipulations of thermodynamics result in the well-known relations

$$c_p > c_v > 0, \tag{2.4}$$

where c_p is the specific heat at constant pressure. The condition that β be positive is not mandated by any general principle but is assumed here for the sake of convenience. Most vapours are expected to satisfy (2.3) although it is known that $\beta < 0$ for some substances, e.g. water at temperatures between 0 °C and 4 °C.

Shock waves are required to satisfy the Rankine–Hugoniot jump conditions:

$$[\rho v] = 0, \tag{2.5}$$

$$\frac{[p]}{[V]} = -m^2, \tag{2.6}$$

$$[h] = [p]\,\frac{V_2 + V_1}{2}, \tag{2.7}$$

where the subscripts 1 and 2 denote properties upstream and downstream of the shock, the square brackets denote the jump in any quantity, i.e.

$$[A] = A_2 - A_1,$$

v is the particle velocity measured in a frame moving with the shock, $V \equiv 1/\rho$ is the specific volume,

$$m \equiv \rho_1 v_1 = \rho_2 v_2 \tag{2.8}$$

is the mass flux and $h(\rho, T)$ is the enthalpy. Equations (2.5)–(2.7) express the principles of conservation of mass, momentum and energy, respectively. A further requirement is that the entropy inequality

$$[s] \geqslant 0 \tag{2.9}$$

be satisfied for all admissible shock waves.

The energy equation (2.7) gives the locus of thermodynamic states which may be connected by a shock wave. We refer to p, V pairs satisfying (2.7) as the Hugoniot curve or shock adiabat. The general form of the adiabat and, in particular, the curvature is of central interest in the present study. A simple proof of the important features is obtained by considering the variation of the entropy along this adiabat:

$$\frac{\mathrm{d}s_2}{\mathrm{d}V_2} = \frac{[V]^2}{2T_2}\frac{\mathrm{d}m^2}{\mathrm{d}V_2}. \tag{2.10}$$

This result is derived by combining Gibbs' relation

$$\mathrm{d}h = T\,\mathrm{d}s + V\,\mathrm{d}p \tag{2.11}$$

with (2.7) and may be found in most standard treatments of gasdynamics, see, e.g. Landau & Lifshitz (1959, §84). Because $\mathrm{d}m^2/\mathrm{d}V_2$ is of order one, at most, as V_2 approaches V_1 we have

$$\frac{\mathrm{d}s_2}{\mathrm{d}V_2} = O([V]^2) \tag{2.12}$$

as V_2 approaches V_1. Relation (2.12) is recognized as a variant of Bethe's relation which states that $[s] = O([V]^3)$ in the weak-shock limit. We now note that the pressure along the shock is given by

$$\frac{\mathrm{d}p_2}{\mathrm{d}V_2} = \left.\frac{\partial p}{\partial V}\right|_s (V_2, s_2) + \frac{\mathrm{d}s_2}{\mathrm{d}V_2}\left.\frac{\partial p}{\partial s}\right|_V (V_2, s_2). \tag{2.13}$$

where $p_2 = p(V_2, s_2) = p(V_2, s_2(V_2))$. In the limit of vanishing shock strength we find

$$\lim_{V_2 \to V_1} \frac{\mathrm{d}p_2}{\mathrm{d}V_2} = \left.\frac{\partial p}{\partial V}\right|_s (V_1, s_1).$$

Use of well-known thermodynamic identities along with (2.2) and (2.4) yields

$$\left.\frac{\partial p}{\partial V}\right|_s = -\rho^2 \left.\frac{\partial p}{\partial \rho}\right|_s = -\rho^2 \gamma \left.\frac{\partial p}{\partial \rho}\right|_T < 0,$$

where $\gamma \equiv c_p/c_v > 1$ is the ratio of specific heats. Thus, the slope of the adiabat $\mathrm{d}p/\mathrm{d}V$ in single-phase gases is necessarily negative for all pressures and temperatures. A similar analysis may be employed to show that the curvature, proportional to

$$\frac{\mathrm{d}^2 p_2}{\mathrm{d}V_2^2} = \frac{\partial^2 p}{\partial V^2} + 2\frac{\mathrm{d}s_2}{\mathrm{d}V_2}\frac{\partial^2 p}{\partial V\,\partial s} + \left(\frac{\partial s_2}{\mathrm{d}V_2}\right)^2 \frac{\partial^2 p}{\partial s^2} + \frac{\mathrm{d}^2 s_2}{\mathrm{d}V_2^2}\frac{\partial p}{\partial s}, \tag{2.14}$$

has the same sign as the local value of Γ. That is,

$$\lim_{V_2 \to V_1} \frac{\mathrm{d}^2 p_2}{\mathrm{d}V_2^2} = \frac{\partial^2 p}{\partial V^2}(V_1, s_1) = \frac{2a_1}{V_1^4}\Gamma(V_1, s_1), \tag{2.15}$$

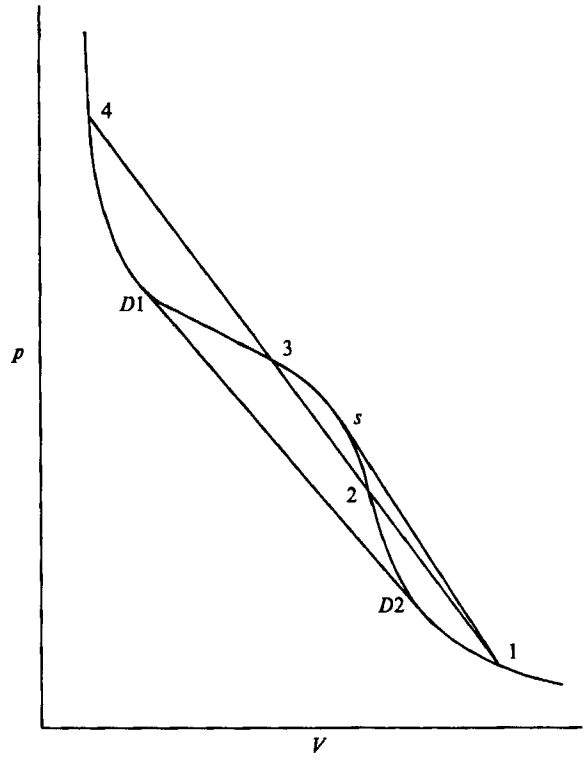

FIGURE 2. Sketch of a typical shock adiabat entering the $\Gamma < 0$ region.

where the subscripts 1 denote quantities evaluated at V_1, s_1. Standard thermodynamic identities were used to relate Γ to $\partial^2 p/\partial V^2$, see, e.g. Thompson (1971), and the derivative of (2.10) was required to show that

$$\frac{\mathrm{d}^2 s_2}{\mathrm{d}V_2^2} = O([V])$$

as V_2 approaches V_1. Thus, the shock adiabat is concave up at every point at which $\Gamma > 0$ and is concave down at every point at which $\Gamma < 0$. The shock adiabat of Bethe–Zel'dovich fluids will therefore be similar to that sketched in figure 2, at least those adiabats which enter the region of negative nonlinearity.

The speed of a shock may be related to the slope of a straight line connecting the upstream and downstream states through the well-known identity

$$M_1 = \frac{V_1}{a_1}\left(-\frac{[p]}{[V]}\right)^{\frac{1}{2}}, \tag{2.16}$$

where $M_1 \equiv v_1/a_1 = mV_1/a_1$ is the shock Mach number. By combining the definition of the Mach number, (2.6)–(2.8) and (2.11), a second identity may be derived which relates the downstream Mach number M_2 to the slope of the chord connecting the upstream and downstream states and the slope of the adiabat. This reads

$$\frac{\mathrm{d}p_2}{\mathrm{d}V_2} - \frac{[p]}{[V]} = \frac{2c_{p2}a_2^2}{V_2}\frac{M_2^2-1}{[V]\beta_2 a_2^2 + 2c_{p2}V_2}. \tag{2.17}$$

We note that the denominator vanishes for compression shocks having

$$\frac{[V]}{V_2} = -2\frac{c_{p2}}{\beta_2 a_2^2}.$$

This is the usual singularity in which p_2 goes to positive infinity as we approach from the right in the (p, V)-diagram. In the case of perfect gases this singularity occurs at $V_2 = V_1(\gamma-1)/(\gamma+1)$. Here we restrict our attention to the region to the right of this singularity, i.e. to shocks having

$$\frac{[V]}{V_2} + \frac{2c_{p2}}{\beta_2 a_2^2} > 0.$$

Relation (2.17) may then be used to show that

$$M_2 \gtreqless 1 \quad \text{whenever} \quad \frac{\mathrm{d}p_2}{\mathrm{d}V_2} \gtreqless \frac{[p]}{[V]} \tag{2.18}$$

and, in particular, tangency points such as s in figure 2 correspond to $M_2 = 1$; this is recognized as a sonic shock. A relation similar to (2.17) may be derived for M_1 from which we may show

$$M_1 \gtreqless 1 \quad \text{whenever} \quad \frac{\mathrm{d}p_1}{\mathrm{d}V_1} \gtreqless \frac{[p]}{[V]}. \tag{2.19}$$

Results (2.18) and (2.19) are useful in that we may determine whether the flow upstream or downstream of a shock is supersonic or subsonic by a simple visual inspection of the shock adiabat.

The sign of the entropy jump may be deduced from the following identity:

$$\int_{s_1}^{s_2} T\,\mathrm{d}s = A_{\mathrm{H}} - A_{\mathrm{c}}, \tag{2.20}$$

where

$$A_{\mathrm{H}} \equiv \int_{V_1}^{V_2} p\,\mathrm{d}V$$

is the area under the shock adiabat from state 1 to 2 and

$$A_{\mathrm{c}} \equiv \frac{p_2+p_1}{2}[V]$$

is the area under the straight line connecting states 1 and 2. A result similar to (2.20) was given by Thompson & Lambrakis (1973). Its derivation combines (2.7) with a straightforward integration of Gibbs' relation (2.11). Because $T > 0$, the sign of $[s]$ is the sign of the integral on the left of (2.20). To illustrate the application of this result we consider shock 2–3 and the double sonic shock $D1$–$D2$ in figure 2. From (2.20) it is clear that both shocks must be expansion shocks in order to satisfy the entropy inequality.

The shock between states 1 and 4 in figure 2 is of particular interest in the present study. As sketched $|A_{\mathrm{c}}| > |A_{\mathrm{H}}|$ which from (2.20) implies that this shock satisfies the entropy inequality only if the upstream state is at 1, i.e. shock 1–4 is a compression shock. Conditions (2.18) and (2.19) show that this corresponds to a supersonic–subsonic transition, i.e. $M_1 > 1 > M_2$. In the next section we show that compression shocks of this type do not possess a dissipative structure and will not remain as a single discontinuity. In §4 these inadmissible discontinuities are shown to result in shock splitting.

3. Dissipative structure

The usual model for the dissipative structure takes the flow to be steady, one-dimensional and governed by the Navier–Stokes equations. The resultant system is a set of three equations expressing conservation of mass, momentum and energy. It is well-known that the first integral of these equations may be written

$$\rho v = m, \tag{3.1}$$

$$(\lambda+2\mu)\,v' = F(v,T) \equiv p-p_i+m(v-v_i), \tag{3.2}$$

$$kT' = G(v,T) \equiv m(e-e_i)+p_i(v-v_i)-\tfrac{1}{2}m(v-v_i)^2, \tag{3.3}$$

where primes denote differentiation with respect to the distance in the flow direction x and the subscripts i denote either the upstream ($i=1$) or downstream ($i=2$) state. The constant m is the mass flux (2.8) and inequalities (2.1) may be employed to show that $\lambda+2\mu>0$. The solutions to (3.1)–(3.3) are required to approach constants as $x\to\pm\infty$. In particular

$$\left.\begin{aligned} T, v &\to T_1, v_1 \quad \text{as} \quad x\to-\infty \\ T, v &\to T_2, v_2 \quad \text{as} \quad x\to\infty. \end{aligned}\right\} \tag{3.4}$$

when (3.4) are applied to (3.1)–(3.3) we find that the Rankine–Hugoniot conditions of the previous section are recovered. In particular, it may be shown that an alternative expression of the jump conditions (2.5)–(2.7) may be taken to be

$$m = \text{constant}, \quad F(v_i,T_i)=0, \quad G(v_i,T_i)=0. \tag{3.5}$$

which follow from the definitions of F and G.

When Γ is strictly positive the shock adiabat is concave up and there are only two roots to (3.5). The existence and uniqueness of a solution curve to (3.1)–(3.3) which satisfies (3.4) was first given by Gilbarg (1951). The corresponding phase plane is sketched in figure 3(*a*). When Γ is strictly negative, the adiabat is concave down and there are again only two singular points in the phase plane. It is a straightforward exercise to extend Gilbarg's arguments to this case; the phase plane for the $\Gamma<0$ case has been worked out and is sketched in figure 3(*b*).

The Rankine–Hugoniot conditions (2.5)–(2.7) or (3.5) have more than two solutions when problems involving mixed nonlinearity are considered, see e.g. figure 2. The corresponding phase plane may be shown to be that sketched in figure 4. The analysis of Gilbarg may be applied to pairs of neighbouring roots to demonstrate the existence and uniqueness of solution curves between neighbouring pairs. However, the new issue raised by the existence of additional roots is whether solution curves exist between non-neighbouring roots. The fact that such solutions are impossible follows from the observation that

$$\left.\frac{\partial F}{\partial T}\right|_v = \left.\frac{\partial p}{\partial T}\right|_\rho = \rho\beta\left.\frac{\partial p}{\partial \rho}\right|_T > 0, \qquad \left.\frac{\partial G}{\partial T}\right|_v = mc_v > 0,$$

where the inequalities follow immediately from (2.2) and (2.3). The $F=F(v,T)$, $G=G(v,T)$ curves are sketched at selected fixed values of v in figure 5. Thus, for every T, v pair outside the $F=0$, $G=0$ curves

$$\frac{\mathrm{d}T}{\mathrm{d}v} = \frac{\lambda+2\mu}{k}\frac{G}{F} > 0. \tag{3.6}$$

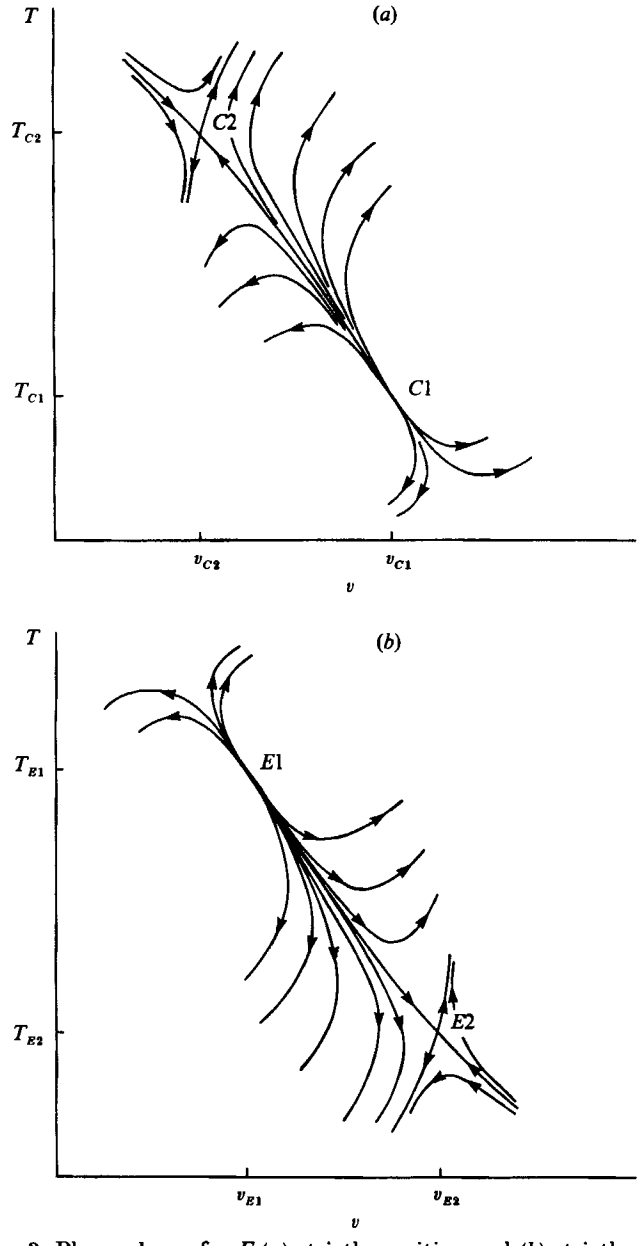

FIGURE 3. Phase planes for Γ (*a*) strictly positive and (*b*) strictly negative.

Because no solution connecting non-neighbouring points may be constructed which satisfies (3.6) (at least one point will have $\mathrm{d}T/\mathrm{d}v < 0$) we conclude that solution curves are only possible between neighbouring roots. A solution starting at any root will inevitably be attracted to the appropriate neighbouring root and will arrive at that root only as $x \to \infty$. Thus, if the chord connecting two shock states p_1, V_1 and p_2, V_2 on an adiabat intersect the adiabat at an intermediate point p_i, V_i, then no dissipative structure may be constructed and the corresponding shock between states 1 and 2 is inadmissible. This is recognized as equivalent to Lax's generalized entropy condition (Lax 1971) which states that the chord connecting acceptable

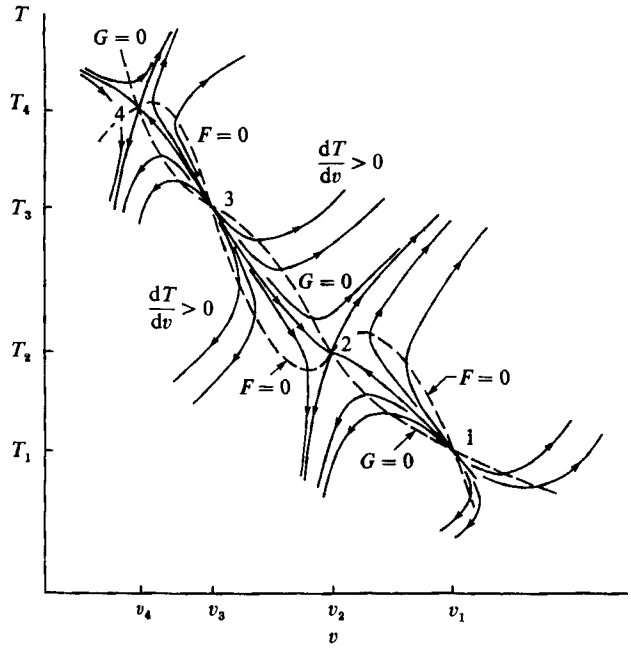

FIGURE 4. Phase plane with mixed nonlinearity. Proposed discontinuity is of the type 1–4 in figure 2.

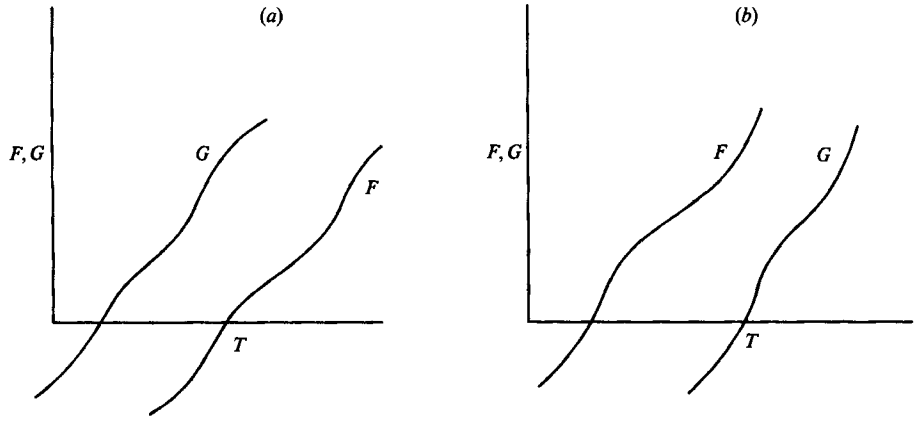

FIGURE 5. Variation of $F(v,T)$ and $G(v,T)$ for fixed v. Case (a) is typical of $v_1 > v > v_2$, $v_3 > v > v_4$, and case (*b*) is typical $v_2 > v > v_3$, $v < v_4$, $v > v_1$ in figure 4.

upstream and downstream states lies entirely above or entirely below the adiabat connecting the same point.

If we consider the upstream state r and corresponding shock adiabat H_1 sketched figure 6, we conclude that unacceptable downstream states are those between $S1$ and M and, of course, those resulting in expansion shocks.

It is of interest to note that upstream and downstream states may be found which satisfy the shock jump conditions and entropy inequality but, owing to the existence of two intermediate intersection points, have no dissipative structure. One example is provided by shock 1–4 in figure 2. A numerical example may be computed for the special case of a van der Waals gas. If c_v is taken to have the constant value $50R$ and the upstream pressure, density and Mach number are given by $0.85p_c$, $0.5\rho_c$ and

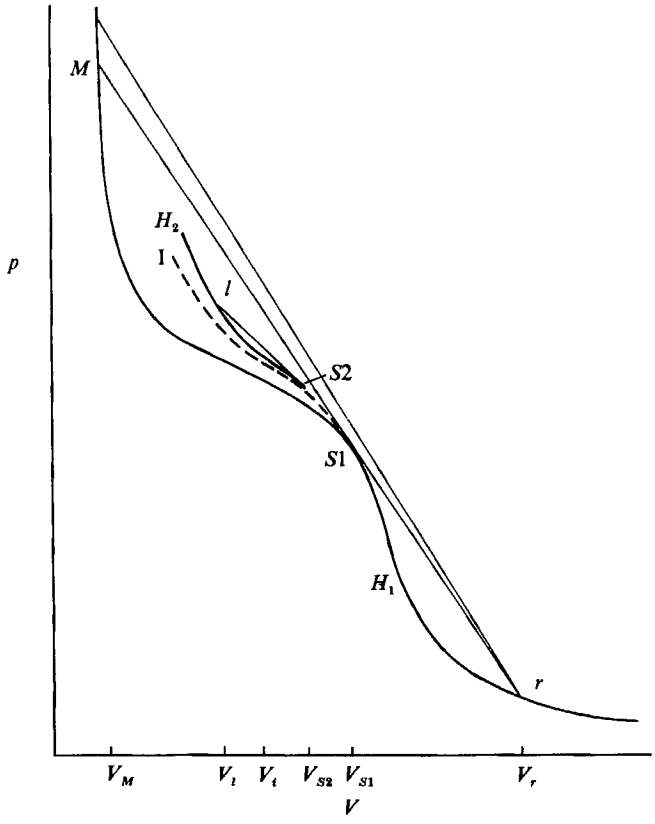

FIGURE 6. Shock adiabats corresponding to shock splitting. H_1 is the shock adiabat fixed by the upstream state r, H_2 is the adiabat of the second shock and the dashed line marked I is the isentrope through $S1$.

1.0124, the downstream pressure, Mach number and entropy jump are calculated to be $1.1p_c$, 0.696, $0.9 \times 10^{-3}R$. It may be shown that the chord connecting these states intersects the adiabat at two intermediate states. Thus, no dissipative structure exists and the shock is inadmissible.

4. Shock splitting

We describe the shock-splitting process through use of a relatively simple initial-value problem. The initial density distributions will be taken to be a series of compressive step functions. In each case, the particle velocity will be taken to be consistent with pure right-moving waves. The undisturbed medium will be taken to be at rest and uniform. The thermodynamic state ahead of (to the right of) the discontinuity will be taken as fixed and will be denoted by the subscript r. The approach will be to demonstrate the wave evolution as the density after the initial discontinuity is increased continuously. The subsequent evolution is plotted in figure 7 and the various shock adiabats and isentropes have been sketched in figure 6.

When the strength of the initial discontinuity is sufficiently small, the shock will be admissible and therefore remain intact. This case corresponds to the weakest shock seen in figure 7. The precise range is $V_{S1} \leqslant V \leqslant V_r$ in the notation of figure 6. When the proposed strength is sufficiently large, the partial disintegration described by Cramer & Kluwick (1984) and Cramer & Sen (1987) occurs. In figure 7 this case

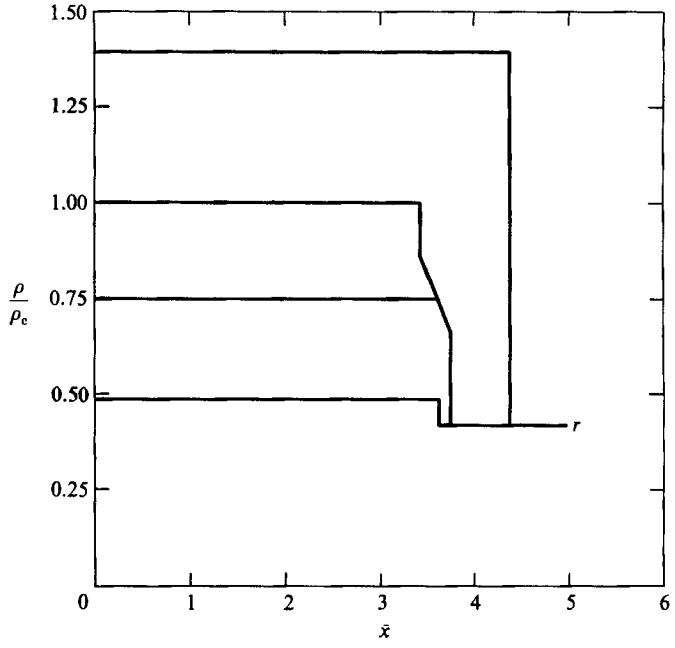

FIGURE 7. Computed density distributions. Gas model is that of van der Waals with $c_v = 50R$. Undisturbed state is at rest and has pressure and density of $0.75p_c$ and $0.42\rho_c$. The horizontal scale is a non-dimensional position. Each distribution corresponds to the same time.

corresponds to the initial condition having a downstream state approximately equal to $0.75\rho_c$. The proposed inadmissible discontinuity is of the type 1–3 in figure 2. The sonic shock is represented by the tangent chord r–$S1$ in figure 6. The thermodynamic states in the compression fan follow the isentrope labelled I in figure 6. Relation (2.10) may be used to show that $S1$ corresponds to a local maximum in $[s]$ on H_1; thus I is tangent to H_1 at $S1$. The fact that I lies above H_1 in the vicinity of $S1$ follows by further noting that the entropy is an increasing function of pressure with constant V; this fact in turn follows by standard thermodynamic manipulations and application of (2.2) and (2.3).

The sonic shock-compression fan structure is correct for all downstream states having $V_t \leqslant V \leqslant V_{S1}$ in the notation of figure 6. Here V_t is the value of V at which the isentrope crosses the $\Gamma = 0$ locus; this corresponds to an inflexion point of the isentrope. The convected sound speed of each point on a right-moving simple wave is given by

$$\sigma = v + a = v_* + a_* + \int_{\rho^*}^{\rho} \Gamma(\rho, s_*)\,\mathrm{d}\rho, \tag{4.1}$$

where the asterisk subscript denotes an appropriate reference state. This result was employed by Cramer & Sen (1987) in a similar initial-value problem and an analogous expression in terms of a pressure integral was also given by Thompson & Lambrakis (1973). Differentiation of (4.1) with respect to density yields

$$\frac{\mathrm{d}\sigma}{\mathrm{d}\rho} = \Gamma(\rho, s_*)$$

which demonstrates that the $\Gamma = 0$ locus also corresponds to a local maximum or minimum of the convected sound speed. Thus, if the strength of the initial

discontinuity exceeds that given by V_i the compression fan curls over to become triple-valued.

In the usual way, the multiple-valued solutions must be replaced by a shock. The upstream state of this shock must always lie in the region of negative nonlinearity. The discussion of §2 demonstrates that the adiabat for this second shock will always be concave down at the upstream state; this adiabat is denoted by H_2 in figure 6. As a result, we may always construct an admissible sonic shock connecting a point on the isentrope in figure 6 to the imposed downstream state V_l, p_l provided $V_M \leqslant V_l \leqslant V_i$. The fact that a downstream state always exists is seen by noting that the adiabat becomes concave up and remains so once H_2 leaves the region of negative nonlinearity. The fact that the entropy rise is always positive is seen by applying (2.20). The choice of a sonic rather than non-sonic shock preserves the self-similar nature of the flow implied by the initial condition. Any other choice would result in a relative motion between the second shock and the compression fan until the sonic condition just assumed is attained. In figure 6, this split-shock configuration is that corresponding to the downstream density of ρ_c, approximately.

As the strength of the initial discontinuity is increased, the second shock becomes stronger with V_{S2} approaching V_{S1} and V_l approaching V_M. When $V_{S2} = V_{S1}$ and $V_l = V_M$, the compression fan disappears and the adiabat of the second shock coincides with that of the original shock. The two shocks then merge to form a single shock. When the strength of the initial discontinuity is increased further, the chord connecting the upstream and downstream states remains above the adiabat, see figure 6, and the initial discontinuity again propagates as a single classical compression shock. An example of this large-amplitude compression shock is that having the downstream density of $1.39\rho_c$, approximately, in figure 7.

In summary, we have shown how to construct solutions for the full range of step-function initial conditions described at the beginning of this section. Both the small- and large-amplitude cases, i.e. those having downstream specific volumes in the range $V_{S1} \leqslant V_l \leqslant V_r$ and $V_l \leqslant V_M$, correspond to admissible shocks and propagate as classical non-sonic compression shocks. As shown in §3, initial conditions for the intermediate cases correspond to inadmissible shocks. When the downstream specific volume lies between V_i and V_{S1} the shock suffers a partial disintegration into a sonic shock and compression fan. A second shock is seen to be required when $V_M \leqslant V_l \leqslant V_i$; this is recognized as shock splitting.

We close this section with a brief description of the computations leading to the plots found in figure 7. The fluid is taken to be a van der Waals gas with constant c_v; thus, the exact solutions for sonic shocks given by Cramer & Sen (1987) may be employed. In particular, the disintegration into a sonic shock–compression fan is just a special case of calculations presented by Cramer & Sen (1987). The split shock is simply two sonic shocks separated by a compression fan. The main difficulty is that each shock lies on a different adiabat. The approach used here was to choose a truncation point for the compression fan of the lower (forerunner) shock. The thermodynamic data at this point (V_{S2}, p_{S2} in figure 6) are combined with the formulas given by Cramer & Sen (1987) to compute the properties of the second shock. The particle velocity ahead of the shock along with the sonic condition is then used to compute the shock position. The non-sonic shocks in figure 7 did not require the solutions of Cramer & Sen (1987). All properties were computed in a straightforward way from the shock adiabat for the van der Waals gas and standard identities.

The numerical data corresponding to the leading sonic shock in the split-shock plot are

$$\frac{\rho_{S1}}{\rho_c} = \frac{2}{3}, \quad \frac{p_{S1}}{p_c} = 0.95, \quad M_1 = 1.06, \quad \frac{[s]}{R} = 7.62 \times 10^{-4},$$

where ρ_{S1} and p_{S1} are the density and pressure immediately following the leading shock, M_1 is the shock Mach number, $[s]$ is the entropy rise and R is the gas constant. The pressure and density immediately before the second shock are $1.015p_c$ and $0.862\rho_c$, respectively. This shock has sonic upstream conditions so that the shock Mach number is unity. After the second shock the pressure, density, and Mach number (computed in a frame moving with the shock) are given by $1.04p_c$, $1.00\rho_c$, and 0.938, respectively. The entropy rise across the second shock was found to be $1.36 \times 10^{-5}R$.

5. Shock formation and evolution

To describe the formation of the split-shock configuration from a smooth density distribution, we consider the ramp-function initial condition sketched in figure 8. The entropy is taken to be uniform and the velocity perturbations are taken to be consistent with simple right-moving waves. Furthermore, the thermodynamic states before and after the transition region, $-\frac{1}{2}L \leqslant x \leqslant \frac{1}{2}L$, are taken to be on opposite sides of the region of negative nonlinearity. The corresponding variation of the fundamental derivative is also sketched in figure 8.

As indicated in §4 the entropy rise associated with shock splitting tends to be small. Even the strongest shock plotted in figure 7 only carries an entropy rise of $4.5 \times 10^{-2}R$. In order to simplify the discussion we shall approximate the flow as isentropic even after shocks form.

A straightforward analysis of the shock formation process may be used to show that the initial density distribution described above steepens to form two compression shocks. A similar analysis of triangle and sine wave initial conditions by the method of characteristics may be found in Cramer & Sen (1986*b*). As depicted in figure 8, these form at the foot of the ramp $\rho = \rho_r$ as well as the top $\rho = \rho_l$ at dimensional times

$$\frac{L}{(\rho_l - \rho_r)\Gamma_r} \quad \text{and} \quad \frac{L}{(\rho_l - \rho_r)\Gamma_l},$$

respectively. Here Γ_r and Γ_l denote the values of the fundamental derivative evaluated at $\rho = \rho_r$ and $\rho = \rho_l$.

After formation each shock increases in strength with the upstream state (ρ_l, s_0) of the lower shock and the downstream state (ρ_r, s_0) of the upper shock remaining fixed; this evolution is depicted in figure 9. In accord with our assumption of isentropic flow and a uniform initial entropy distribution all states will lie on the same isentrope $s = s_0$. If the change in density across the ramp is sufficiently small, i.e. if ρ_r and ρ_l are sufficiently close to the $\Gamma = 0$ locus depicted in figure 1 or, equivalently, the inflexion points of the isentrope, each shock eventually becomes sonic. These are denoted by the tangent chords r–$S1$ and $S2$–l in figure 9(*a*). Any further increase in strength results in a violation of the admissibility condition described in §3, i.e. the chord connecting the upstream and downstream states no longer remain completely above the adiabat. Physically, the portion of the isentropic compression behind the

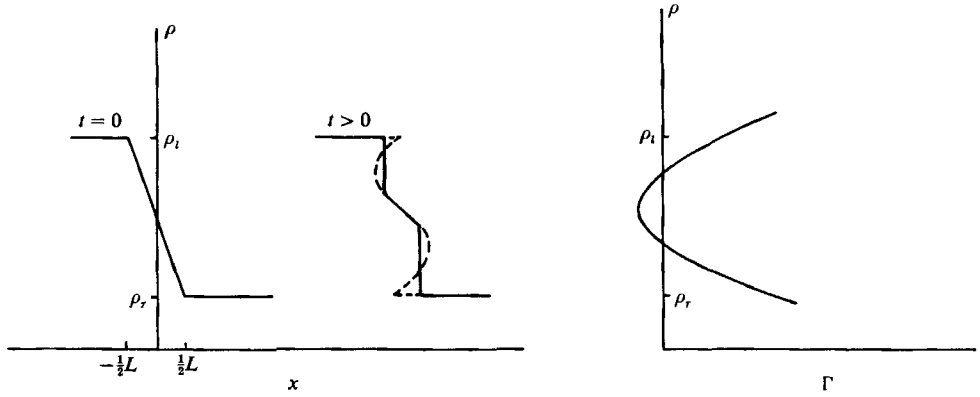

FIGURE 8. Evolution of a smooth density distribution. In the $t > 0$ sketch shocks are used to eliminate multiple-valued solutions. Maximum and minimum propagation speeds correspond to zeros of Γ.

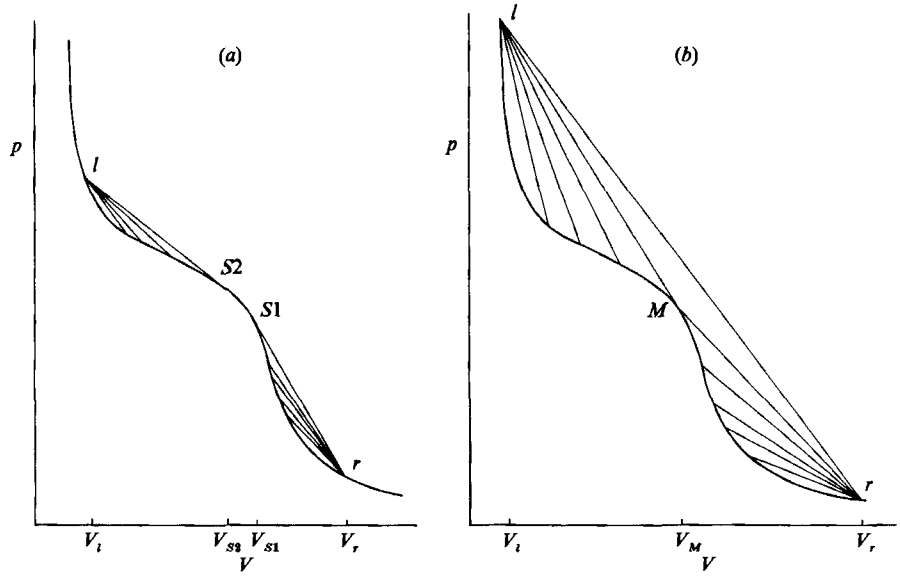

FIGURE 9. Schematic of isentropic shock evolution. (*a*) Shock splitting, (*b*) shock merging.

forerunner shock cannot catch this shock and therefore increase its strength. In like manner, the convected sound speed ahead of the trailing shock is larger than that of the trailing shock after it becomes sonic. Thus, the final result is the split-shock configuration described in §4.

If ρ_l and ρ_r are sufficiently far from the $\Gamma = 0$ locus, the two shocks collide. We note that it is possible, although not necessary, that one of the shocks may become sonic before collision. However, the other will always collide with the sonic shock before becoming sonic itself. In figure 9(*b*) the forerunner shock is denoted by r–M and the trailing shock by M–l at the collision time. After collision the shocks merge into a single large-amplitude compression shock taking the flow from ρ_r to ρ_l. The shock collision and subsequent merging will occur whenever a straight line connecting states l and r remains above the adiabat. Otherwise, the final configuration will be that of shock splitting. Thus, the conclusions based on shock formation are completely consistent with those based on the dissipative structure and the shock

construction process described in the previous section. Furthermore, we have demonstrated that the shock splitting is not just a possible state, but is the inevitable result of the evolution from a smooth initial condition, at least within the context of our isentropic approximation.

6. Summary

The main goal of the present study is to demonstrate that single-phase fluids of the Bethe–Zel'dovich type exhibit shock splitting and to provide exact solutions for van der Waals gases. Furthermore, in §3 we have shown that discontinuities of the type 1–4 in figure 2 have no dissipative structure; the discussions of §§4 and 5 show that such discontinuities break up into the split-shock configuration to provide the transition between the fixed upstream state and the imposed density, pressure or particle velocity downstream. Shock splitting is therefore seen to play the same role as the partial and total disintegrations found in previous investigations, viz. the split shock configurations evolve dynamically from inadmissible discontinuities. The analogue in the theory of perfect gases is the total disintegration of expansion shocks to form centred expansion fans.

Shock splitting has also been observed in two-phase flows, see e.g. Thompson & Kim (1983) and Thompson *et al.* (1987). There are a number of interesting parallels with the present study, particularly in Thompson's equilibrium model. For example, the effective region of negative nonlinearity produced by the kink in the adiabats, the shock construction procedure and predictions of merged shocks all have analogues here. An important distinction is that the shocks found in the present study are all gasdynamic shocks in the single-phase region rather than the shock-condensation wave structures found by Thompson and co-workers. The occurrence of shock splitting in sedimentation waves has also been predicted by Kynch (1952) and realized in the experiments of Shannon & Tory (1965). The author is indebted to one of the referees for pointing out the latter reference.

The existence issues discussed in §§4 and 5 are valid for both steady and unsteady flows. We also anticipate that the details of the partial disintegration and shock splitting have analogues in steady flow configurations. Two advantages of the tendency to limit the strength of compression shocks in steady flows immediately come to mind. The first is that the losses in stagnation pressure and those due to wave drag are minimized owing to a reduction of the irreversible portion of the compression. Furthermore, Cramer & Kluwick (1984) have shown that the entropy rise across weak sonic shocks will be an order of magnitude smaller than normally predicted. Thus, we expect that even the shocks which remain will result in a minimum of loss. Important losses in many transonic and supersonic internal flows are due to shock-induced separation. Thus, the second advantage of the disintegration process is the drastic reduction in the adverse pressure gradient. Future studies will attempt to determine whether the shock-limiting mechanism and others inherent in Bethe–Zel'dovich fluids can be exploited to increase the efficiency of turbomachinery and other flows involving dense gases.

REFERENCES

BETHE, H. A. 1942 The theory of shock waves for an arbitrary equation of state. *Office Sci. Res. & Dev. Rep.* 545.

CRAMER, M. S. 1987*a* Structure of weak shocks in fluids having embedded regions of negative nonlinearity. *Phys. Fluids* **30**, 3034–3044.

CRAMER, M. S. 1987*b* Dynamics of shock waves in certain dense gases. In *Proc. 16th Intl Symp. on Shock Tubes and Waves, Aachen, West Germany*, pp. 139–144.

CRAMER, M. S. 1987*c* Dynamics of shock waves in gases having large specific heats. In *Proc. 20th Midwestern Mechanics Conf., Purdue University, W. Lafayette, Indiana*, pp. 207–211.

CRAMER, M. S. & KLUWICK, A. 1984 On the propagation of waves exhibiting both positive and negative nonlinearity. *J. Fluid Mech.* **142**, 9–37.

CRAMER, M. S., KLUWICK, A., WATSON, L. T. & PELZ, W. 1986 Dissipative waves in fluids having both positive and negative nonlinearity. *J. Fluid Mech.* **169**, 323–336.

CRAMER, M. S. & SEN, R. 1986*a* Sonic shocks in certain dense gases. *Bull. Am. Phys. Soc.* **31**, 1720.

CRAMER, M. S. & SEN, R. 1986*b* Shock formation in fluids having embedded regions of negative nonlinearity. *Phys. Fluids* **29**, 2181–2191.

CRAMER, M. S. & SEN, R. 1987 Exact solutions for sonic shocks in van der Waals gases. *Phys. Fluids* **30**, 377–385.

GILBARG, D. 1951 The existence and limit behavior of the one-dimensional shock layer. *Am. J. Maths* **73**, 256–274.

KYNCH, G. J. 1952 A theory of sedimentation. *Trans. Faraday Soc.* **48**, 166–176.

LAMBRAKIS, K. & THOMPSON, P. A. 1972 Existence of real fluids with a negative fundamental derivative Γ. *Phys. Fluids* **5**, 933–935.

LANDAU, L. D. & LIFSHITZ, E. M. 1959 *Fluid Mechanics*. Addison-Wesley.

LAX, P. D. 1971 Shock waves and entropy. In *Contributions to Nonlinear Functional Analysis* (ed. E. H. Zarantonello). Academic.

LEE-BAPTY, I. P. 1981 Nonlinear wave propagation in stratified and viscoelastic media. Ph.D. dissertation, Leeds University, England.

LEE-BAPTY, I. P. & CRIGHTON, D. G. 1987 Nonlinear wave motion governed by the modified Burger's equation. *Phil. Trans. R. Soc. Lond.* A **323**, 173–209.

SHANNON, P. T. & TORY, E. M. 1965 Settling of slurries. *Ind. Engng Chem.* **57**, 18–25.

THOMPSON, P. A. 1971 A fundamental derivative in gasdynamics. *Phys. Fluids.* **14**, 1843–1849.

THOMPSON, P. A., CHAVES, H., MEIER, G. E. A., KIM, Y.-G. & SPECKMANN, H.-D. 1987 Wave splitting in a fluid of large heat capacity. *J. Fluid Mech.* **185**, 385–414.

THOMPSON, P. A. & KIM, Y.-G. 1983 Direct observation of shock splitting in a vapor–liquid system. *Phys. Fluids* **26**, 3211–3215.

THOMPSON, P. A. & LAMBRAKIS, K. 1973 Negative shock waves. *J. Fluid Mech.* **60**, 187–208.

TURNER, T. N. 1979 Second-sound shock waves and critical velocities in liquid helium II. Ph.D. Dissertation, California Institute of Technology, Pasadena, Ca.

TURNER, T. N. 1981 New experimental results obtained with second-sound shock waves. *Physica* **107B**, 701–702.

ZEL'DOVICH, YA. B. 1946 On the possibility of rarefaction shock waves. *Zh. Eksp. Teor. Fiz.* **4**, 363–364.